A Branch Cut Type Sign Estimator for Single-Frame Fringe Projection Profilometry

Daichi KITAHARA† Isao YAMADA†
†Department of Communications and Computer Engineering, Tokyo Institute of Technology

Abstract In the last two decades, for three-dimensional (3D) measurement of moving objects, estimation of the continuous phase, which corresponds to 3D surface information, from a single fringe image has been a challenging problem. Differently from standard fringe projection using at least three fringe images for 3D measurement of static objects, we have to estimate the sign function of the sine of the continuous phase before two-dimensional (2D) phase unwrapping. In this paper, we newly formulate the sign estimation problem as a minimization problem for a certain energy of local change of the continuous phase. For solving this combinatorial optimization problem, we propose a branch cut type algorithm which is inspired by Goldstein's combinatorial approach to 2D phase unwrapping. Numerical experiments demonstrate that the proposed sign estimator achieves higher estimation accuracy than a state-of-the-art estimator.

1 Introduction

Fringe projection is a major technique to obtain three-dimensional (3D) information of objects in a non-contact manner [1]–[3], and widely used in biomedical [4]–[6], industrial [7]–[9], kinematics [10], [11], and biometric [12], [13] applications. A typical fringe projection profilometry system is illustrated in Fig. 1. It consists of a projector, a camera and a digital computer. First, the projector projects sinusoidal fringe patterns onto an object. Second, the camera records intensity images of the fringe patterns which are distorted due to the surface profile of the object. Third, from the recorded images, the digital computer estimates the continuous phase distribution which corresponds to the horizontal projector pixels by using some fringe analysis composed of *wrapped phase detection* and *phase unwrapping* steps. Finally, a 3D surface is computed from the camera pixels and the projector pixels on the basis of triangulation.

A most popular fringe projection technique is the *phase-shifting method (PSM)* [14] because it can obtain 3D information stably from at least three simple fringe images as follows. Three fringe images I_k $(k = 1, 2, 3)$, whose phases are shifted by $2\pi/3$ from each other, are recorded on two-dimensional (2D) lattice points $(x, y) \in \mathcal{L}$ as

$$\left.\begin{aligned} I_1(x,y) &= a(x,y) + b(x,y)\cos(\phi(x,y)) + n_1(x,y) \\ I_2(x,y) &= a(x,y) + b(x,y)\cos(\phi(x,y) - \tfrac{2\pi}{3}) + n_2(x,y) \\ I_3(x,y) &= a(x,y) + b(x,y)\cos(\phi(x,y) + \tfrac{2\pi}{3}) + n_3(x,y) \end{aligned}\right\}, \tag{1}$$

where $\mathcal{L}$ is the set of all lattice points captured by the camera, a is a slowly varying background illumination, b is the fringe amplitude that is also a low-frequency signal, ϕ is the continuous phase distribution (the so-called *unwrapped phase*) to be estimated, and n_k $(k = 1, 2, 3)$ are independent additive noises. The *wrapped phase*

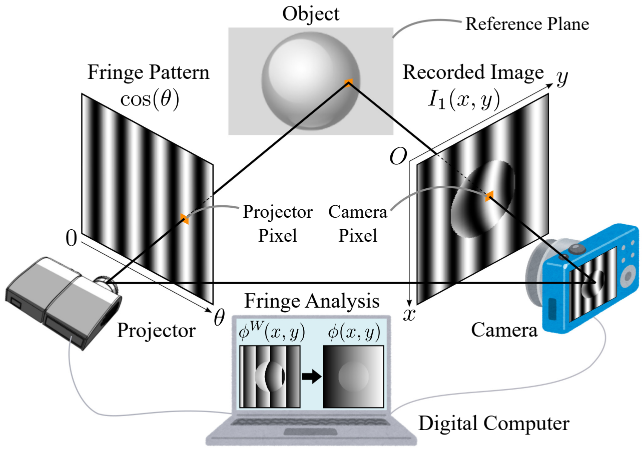

Figure 1: Typical fringe projection profilometry system.

$$\phi^W(x,y) := W(\phi(x,y) + \nu(x,y)) \in (-\pi, \pi] \tag{2}$$

is computed by using $\cos(\phi^W) = \frac{2I_1 - I_2 - I_3}{\sqrt{(2I_1-I_2-I_3)^2 + 3(I_2-I_3)^2}}$ and $\sin(\phi^W) = \frac{\sqrt{3}(I_2-I_3)}{\sqrt{(2I_1-I_2-I_3)^2+3(I_2-I_3)^2}}$, where $\nu \in (-\pi, \pi]$ is phase noise and $W : \mathbb{R} \to (-\pi, \pi]$ is the *wrapping operator* defined by

$$\forall \varphi \in \mathbb{R}\ \exists \eta \in \mathbb{Z} \quad \varphi = W(\varphi) + 2\pi\eta \text{ and } W(\varphi) \in (-\pi, \pi].$$

ϕ is estimated from ϕ^W by 2D phase unwrapping [15]–[18], and a 3D surface corresponding to the camera pixel $(x, y) \in \mathcal{L}$ is obtained from the horizontal projector pixel $\theta = \phi(x, y)$ on the basis of triangulation.

However, PSM requires that the physical quantities a, b and ϕ remain constant during the time needed to record the images I_k $(k = 1, 2, 3)$, i.e., a, b and ϕ must be common for all indices $k = 1, 2, 3$ in (1). This condition is hardly satisfied when the measurement is for transient phenomena [19] or the environment is hostile. To deal with such situations, reconstruction of ϕ from a single fringe image I_1 in (1) has been challenged, and several phase recovery algorithms have been proposed [19]–[25]. These algorithms usually use a high pass filter [20] to remove the background illumination a, and then use Hilbert transform [26] to normalize the fringe amplitude b. As a result, the normalized fringe image is generated from I_1 as

$$I(x,y) = \cos(\phi(x,y) + \nu(x,y)) \in [-1, 1]. \tag{3}$$

From (2) and (3), the absolute value of the wrapped phase is computed as

$$|\phi^W(x,y)| = \arccos(I(x,y)) \in [0,\pi].$$

Therefore, the key to compute $\phi^W(x,y)$ for all $(x,y) \in \mathcal{L}$ is reliable estimation of the sign in

$$\phi^W(x,y) = \mathrm{sgn}(\phi^W(x,y))|\phi^W(x,y)|, \tag{4}$$

where $\mathrm{sgn}(t) := +1$ for $t \geq 0$ and $\mathrm{sgn}(t) := -1$ for $t < 0$.

In this paper, we newly formulate a minimization problem for a certain energy of local change of ϕ so that we use a minimizer of the energy as an estimate of $\mathrm{sgn}(\phi^W(x,y))$ (see Section 2.1). To solve this combinatorial optimization problem, we propose a branch cut type algorithm in Section 3 which is inspired by Goldstein's combinatorial approach to 2D phase unwrapping[1] [17] (see Section 2.2). Numerical experiments in Section 4 demonstrate that the proposed method provides a remarkable improvement over an existing path-following method [23]. Finally, in Section 5, we conclude this paper.

2 Preliminaries

Let $\mathbb{Z}$, $\mathbb{R}$ and $\mathbb{R}_+$ be respectively the set of all integers, real numbers and nonnegative real numbers. Boldface small letters express vectors, and boldface capital letters express matrices. The norm of $\boldsymbol{x} := (x_1, x_2, \ldots, x_n)^T \in \mathbb{R}^n$ is defined as $\|\boldsymbol{x}\| := \sqrt{\sum_{i=1}^n x_i^2}$. In what follows, let $\mathcal{L} := \{(x_i, y_j)\}_{j=1,2,\ldots,n}^{i=1,2,\ldots,m}$ s.t. $x_1 < x_2 < \cdots < x_m$ and $y_1 < y_2 < \cdots < y_n$. For any function f define on $\Omega := [x_1, x_m] \times [y_1, y_n]$, we use notation $f_{i,j} := f(x_i, y_j)$.

2.1 Energy Minimization for Sign Ambiguity Resolution

Assuming that the normalized image I in (3) is noise-free, i.e., $\nu(x,y) = 0 \ \forall(x,y) \in \Omega$, the image gradient $\nabla I(x,y) := (\frac{\partial I}{\partial x}(x,y), \frac{\partial I}{\partial y}(x,y))^T$ and the unwrapped phase gradient $\nabla \phi(x,y) := (\frac{\partial \phi}{\partial x}(x,y), \frac{\partial \phi}{\partial y}(x,y))^T$ satisfy

$$\nabla I(x,y) = -\sin(\phi(x,y))\nabla\phi(x,y).$$

Therefore, the orientation of $\nabla\phi(x,y)$ is the same as or opposite to that of $\nabla I(x,y)$ depending on $s(x,y) := \mathrm{sgn}(W(\phi(x,y))) = \mathrm{sgn}(\sin(\phi(x,y)))$. On the basis of the idea of *functional data analysis* [18], [27], i.e., minimization of the energy of local change of ϕ:

$$\begin{aligned}
&\iint_\Omega \left[\left|\frac{\partial^2\phi}{\partial x^2}\right|^2 + 2\left|\frac{\partial^2\phi}{\partial x \partial y}\right|^2 + \left|\frac{\partial^2\phi}{\partial y^2}\right|^2\right] \mathrm{d}x\mathrm{d}y \\
&\approx \sum_{i=1}^{m}\sum_{j=1}^{n-1} \|\nabla\phi(x_i, y_{j+1}) - \nabla\phi(x_i,y_j)\|^2 \\
&\quad + \sum_{i=1}^{m-1}\sum_{j=1}^{n} \|\nabla\phi(x_{i+1}, y_j) - \nabla\phi(x_i,y_j)\|^2,
\end{aligned}$$

we newly introduce Problem 1 below, which is similar to the optimization problem proposed in [19] for estimation of $s_{i,j}$.

[1]For higher resolution in 2D phase unwrapping, see an algebraic approach [18] which is robust against the measurement errors.

Problem 1 (Approximated energy minimization problem) *Find $\boldsymbol{S}^* := (s^*_{i,j}) \in \{-1,+1\}^{m\times n}$ minimizing*

$$\begin{aligned}
J(\boldsymbol{S}) := &\sum_{i=1}^{m}\sum_{j=1}^{n-1} \|s_{i,j+1}\boldsymbol{v}_{i,j+1} - s_{i,j}\boldsymbol{v}_{i,j}\|^2 \\
&+ \sum_{i=1}^{m-1}\sum_{j=1}^{n} \|s_{i+1,j}\boldsymbol{v}_{i+1,j} - s_{i,j}\boldsymbol{v}_{i,j}\|^2,
\end{aligned} \tag{5}$$

where $\boldsymbol{v}_{i,j} := \frac{\nabla I(x_i,y_j)}{\|\nabla I(x_i,y_j)\|}$ ($i = 1,2,\ldots,m$ and $j = 1,2,\ldots,n$) are the normalized image gradient vectors at (x_i,y_j), and $\nabla I(x_i,y_j)$ are approximately computed by applying, e.g., the Prewitt or the Sobel operator, to I in (3).

After finding a minimizer $\boldsymbol{S}^* = (s^*_{i,j})$, from (4) and $\phi^W_{i,j} \neq -\pi$, the wrapped phase $\phi^W_{i,j}$ is estimated by

$$\phi^W_{i,j} = \begin{cases} |\phi^W_{i,j}| & \text{if } |\phi^W_{i,j}| = 0 \text{ or } |\phi^W_{i,j}| = \pi; \\ s^*_{i,j}|\phi^W_{i,j}| & \text{otherwise.} \end{cases}$$

Remark 1 *There are at least two minimizers of (5) because $J(\boldsymbol{S}) = J(-\boldsymbol{S})$ for any $\boldsymbol{S} \in \{-1,+1\}^{m\times n}$. Actually, we need other information to judge which minimizer should be used for the above wrapped phase estimation.*

2.2 Goldstein's Branch Cut for 2D Phase Unwrapping

All commonly used 2D phase unwrapping algorithms assume that $\phi_{i,j+1} - \phi_{i,j} \in (\pi,\pi]$, $\phi_{i+1,j} - \phi_{i,j} \in (\pi,\pi]$, and $|\nu_{i,j}|$ is small for most i and j. To reconstruct $\phi_{i,j}$ satisfying the above assumption, Goldstein et al. proposed the following branch cut algorithm [17].

1. Detect every closed loop $\mathrm{CL}_{i,j} := ((x_i,y_j) \to (x_i,y_{j+1}) \to (x_{i+1},y_{j+1}) \to (x_{i+1},y_j) \to (x_i,y_j))$ having a nonzero *residue* by discretized contour integrals:

$$\begin{aligned}
r_{i,j} &:= \frac{1}{2\pi}\Big(W\big(\phi^W_{i,j+1} - \phi^W_{i,j}\big) + W\big(\phi^W_{i+1,j+1} - \phi^W_{i,j+1}\big) \\
&\qquad - W\big(\phi^W_{i+1,j+1} - \phi^W_{i+1,j}\big) - W\big(\phi^W_{i+1,j} - \phi^W_{i,j}\big)\Big) \\
&= \begin{cases} 0 & (\mathrm{CL}_{i,j} \text{ has no residue}); \\ \pm 1 & (\mathrm{CL}_{i,j} \text{ has a positive/negative residue}). \end{cases}
\end{aligned} \tag{6}$$

   Mark the center of such $\mathrm{CL}_{i,j}$ with ± 1 (see Fig. 2(a)).
2. Create *branches* as shown in Fig. 2(b). Each branch is defined as a path connecting the same number of positive residues and negative residues, or the residues and the outside of Ω.
3. Construct the unwrapped phase $\phi_{i,j}$ based on the branches by satisfying $\phi_{1,1} = \phi^W_{1,1} + 2\pi\eta_{1,1}$ ($\eta_{1,1} \in \mathbb{Z}$),

$$\phi_{i,j+1} - \phi_{i,j} = W\big(\phi^W_{i,j+1} - \phi^W_{i,j}\big) \in (\pi,\pi]$$

   if there is no branch between (x_i,y_j) and (x_i,y_{j+1}), and

$$\phi_{i+1,j} - \phi_{i,j} = W\big(\phi^W_{i+1,j} - \phi^W_{i,j}\big) \in (\pi,\pi]$$

   if there is no branch between (x_i,y_j) and (x_{i+1},y_j). This algorithm guarantees $W(\phi_{i,j}) = \phi^W_{i,j}$ for all $i = 1,2,\ldots,m$ and $j = 1,2,\ldots,n$ (see Fig. 2(b)).

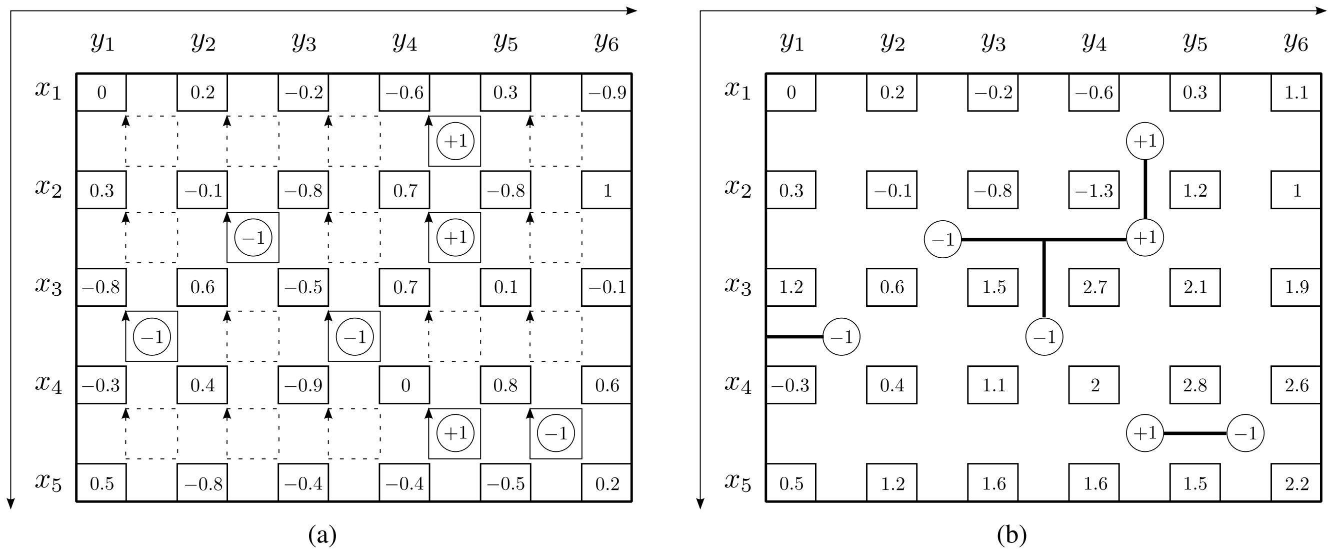

Figure 2: Illustration of the idea of Goldstein's branch cut [17] for 2D phase unwrapping: (a) detection of every closed loop having a nonzero residue $r_{i,j} = \pm 1$ in (6) from given normalized wrapped phase $\phi^W_{i,j}/\pi$ ($i = 1, 2, \ldots, 5$ and $j = 1, 2, \ldots, 6$) and (b) construction of branches and corresponding unwrapped phase $\phi_{i,j}/\pi$ ($i = 1, 2, \ldots, 5$ and $j = 1, 2, \ldots, 6$).

3 Branch Cut Type Sign Estimator

3.1 Reformulation of Problem 1

In (5), let $J^h_{i,j}(s_{i,j}, s_{i,j+1}) := \|s_{i,j+1}\boldsymbol{v}_{i,j+1} - s_{i,j}\boldsymbol{v}_{i,j}\|^2$ and $J^v_{i,j}(s_{i,j}, s_{i+1,j}) := \|s_{i+1,j}\boldsymbol{v}_{i+1,j} - s_{i,j}\boldsymbol{v}_{i,j}\|^2$. Then $J^h_{i,j}$ and $J^v_{i,j}$ depend only sign changes between neighboring pairs $(s_{i,j}, s_{i,j+1})$ and $(s_{i,j}, s_{i+1,j})$, respectively. For each sign matrix $\boldsymbol{S} = (s_{i,j}) \in \{-1, +1\}^{m\times n}$, by defining sign change matrices $\boldsymbol{C}_h = (c^h_{i,j}) \in \{0, 1\}^{m\times(n-1)}$ and $\boldsymbol{C}_v = (c^v_{i,j}) \in \{0, 1\}^{(m-1)\times n}$ as

$$c^h_{i,j} := \begin{cases} 0 & \text{if } s_{i,j+1} = s_{i,j}; \\ 1 & \text{if } s_{i,j+1} = -s_{i,j}, \end{cases} \tag{7}$$

and

$$c^v_{i,j} := \begin{cases} 0 & \text{if } s_{i+1,j} = s_{i,j}; \\ 1 & \text{if } s_{i+1,j} = -s_{i,j}, \end{cases} \tag{8}$$

and by defining new cost functions $\hat{J}^h_{i,j} : \{0, 1\} \to \mathbb{R}_+$ and $\hat{J}^v_{i,j} : \{0, 1\} \to \mathbb{R}_+$ as

$$\begin{cases} \hat{J}^h_{i,j}(0) := J^h_{i,j}(+1, +1) = J^h_{i,j}(-1, -1); \\ \hat{J}^h_{i,j}(1) := J^h_{i,j}(+1, -1) = J^h_{i,j}(-1, +1), \end{cases}$$

and

$$\begin{cases} \hat{J}^v_{i,j}(0) := J^v_{i,j}(+1, +1) = J^v_{i,j}(-1, -1); \\ \hat{J}^v_{i,j}(1) := J^v_{i,j}(+1, -1) = J^v_{i,j}(-1, +1), \end{cases}$$

we reformulate Problem 1 as Problem 2 below.

Problem 2 (Alternative expression of Problem 1) *Find* $(\boldsymbol{C}^*_h, \boldsymbol{C}^*_v) \in \{0, 1\}^{m\times(n-1)} \times \{0, 1\}^{(m-1)\times n}$ *minimizing*

$$\hat{J}(\boldsymbol{C}_h, \boldsymbol{C}_v) := \sum_{i=1}^{m}\sum_{j=1}^{n-1} \hat{J}^h_{i,j}(c^h_{i,j}) + \sum_{i=1}^{m-1}\sum_{j=1}^{n} \hat{J}^v_{i,j}(c^v_{i,j})$$

subject to

$$c^h_{i,j} \oplus c^v_{i,j+1} \oplus c^h_{i+1,j} \oplus c^v_{i,j} = 0 \tag{9}$$

for all $i = 1, 2, \ldots, m-1$ *and* $j = 1, 2, \ldots, n-1$, *where* $\oplus$ *denotes the exclusive disjunction, i.e.,* $0 \oplus 0 = 1 \oplus 1 = 0$ *and* $0 \oplus 1 = 1 \oplus 0 = 1$ *hold.*

3.2 Branch Cut Type Algorithm for Solving Problem 2

To solve Problem 2 approximately, we present the following branch cut type algorithm, which consists of steps similar to *residue detection* and *branch construction* steps in Goldstein's branch cut [17] developed for 2D phase unwrapping (see Section 2.2). In what follows, assume $\hat{J}^h_{i,j}(0) \neq \hat{J}^h_{i,j}(1)$ and $\hat{J}^v_{i,j}(0) \neq \hat{J}^v_{i,j}(1)$ for all i and j.

1. Define $c^{h,\min}_{i,j} := \operatorname{argmin}_{c\in\{0,1\}} \hat{J}^h_{i,j}(c)$ and $c^{v,\min}_{i,j} := \operatorname{argmin}_{c\in\{0,1\}} \hat{J}^v_{i,j}(c)$ as *locally ideal sign changes*. Detect every $\mathrm{CL}_{i,j}$ satisfying
$$c^{h,\min}_{i,j} \oplus c^{v,\min}_{i,j+1} \oplus c^{h,\min}_{i+1,j} \oplus c^{v,\min}_{i,j} = 1. \tag{10}$$
Mark the center of such $\mathrm{CL}_{i,j}$ (see Fig. 3(a)).
2. Create *branches* as shown in Fig. 3(b). Each branch is defined as a path connecting two centers marked in the first step, or one center and the outside of Ω.
3. Construct sign change matrices $\boldsymbol{C}_h$ and $\boldsymbol{C}_v$ satisfying condition (9) by defining
$$c^h_{i,j} := \begin{cases} c^{h,\min}_{i,j} & \text{if } \begin{cases} \text{there is no branch between} \\ (x_i, y_j) \text{ and } (x_i, y_{j+1}); \end{cases} \\ c^{h,\min}_{i,j} \oplus 1 & \text{otherwise,} \end{cases}$$
and
$$c^v_{i,j} := \begin{cases} c^{v,\min}_{i,j} & \text{if } \begin{cases} \text{there is no branch between} \\ (x_i, y_j) \text{ and } (x_{i+1}, y_j); \end{cases} \\ c^{v,\min}_{i,j} \oplus 1 & \text{otherwise.} \end{cases}$$
Construct a sign matrix $\boldsymbol{S}$ corresponding to sign change matrices $\boldsymbol{C}_h$ and $\boldsymbol{C}_v$ by using relations (7) and (8) (see Fig. 3(b)).

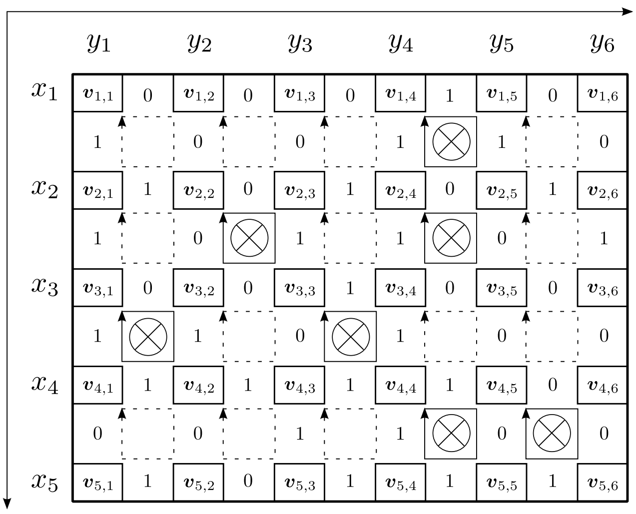

(a)

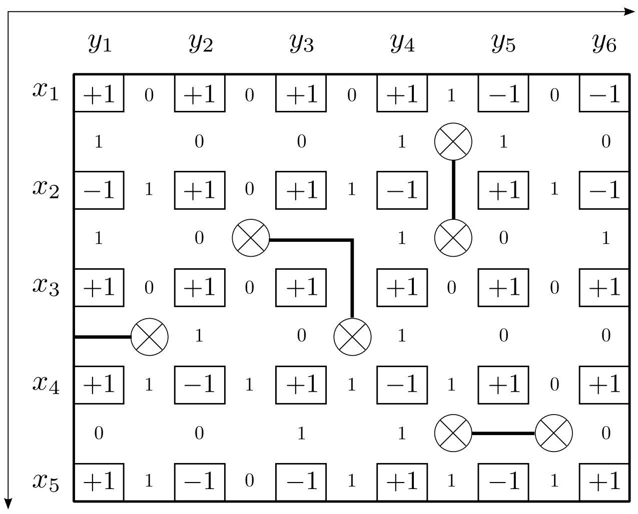

(b)

Figure 3: Illustration of the idea of the proposed branch cut type sign estimator: (a) detection of every closed loop satisfying (10) by using the locally ideal sign changes $c_{i,j}^{h,\min}$ and $c_{i,j}^{h,\min}$ computed from $\boldsymbol{v}_{i,j}$ ($i = 1, 2, \ldots, 5$ and $j = 1, 2, \ldots, 6$) and (b) constructions of branches, sign changes $c_{i,j}^{h}$ and $c_{i,j}^{v}$, and corresponding signs $s_{i,j}$ ($i = 1, 2, \ldots, 5$ and $j = 1, 2, \ldots, 6$).

4 Numerical Experiments

We compare the effectiveness of the proposed sign estimator with that of an existing path-following sign estimator [23] for two objects shown in Figs. 4(a) and 5(a). In both experiments, we set $\mathcal{L} := \{(x_i, y_j)\}_{j=1,2,\ldots,256}^{i=1,2,\ldots,256}$, and set $a(x, y) = 2$, $b(x, y) = 1$, and $n_1(x, y) = 0$ for all $(x, y) \in \mathcal{L}$ in (1). We generate the normalized fringe image $I(x, y)$ by subtracting $\frac{1}{65536}\sum_{i=1}^{256}\sum_{j=1}^{256} I_1(x_i, y_j)$ from $I_1(x, y)$ followed by the normalization into $[-1, 1]$.

Figure 4(b) shows[2] the normalized fringe image $I(x, y)$ based on the object in Fig. 4(a). Figure 4(c) shows the true sign $s(x, y) = \mathrm{sgn}(W(\phi(x, y)))$, to be estimated (see Section 2.1), of the noiseless wrapped phase $W(\phi(x, y))$ in Fig. 4(f). Figures 4(d) and 4(g) respectively depict the sign and the wrapped phase estimated by the algorithm in [23] using the parameters $\mu = 1$ and $\Gamma = 11$. Figures 4(e) and 4(h) respectively depict the sign and the wrapped phase estimated by the proposed method, where we construct branches by repeatedly connecting the closest pair of centers of closed loops satisfying (10). From these figures, we observe that the proposed branch cut type sign estimator achieves lower error rate ($\frac{190}{65536} \approx 0.29\%$) compared with the existing method [23] ($\frac{1053}{65536} \approx 1.61\%$) especially around the edges of the object.

Figure 5(b) shows $I(x, y)$ for the other object ("teapot" provided in MATLAB®) in Fig. 5(a). Figure 5(c) shows the sign $s(x, y)$ of $W(\phi(x, y))$ in Fig. 5(f). Figures 5(d) and 5(g) depict the sign and the wrapped phase estimated by the algorithm in [23]. Figures 5(e) and 5(h) depict the sign and the wrapped phase estimated by the proposed method. In this experiment, the proposed sign estimator achieves again lower error rate ($\frac{141}{65536} \approx 0.22\%$) compared with the existing method [23] ($\frac{1167}{65536} \approx 1.78\%$).

[2]For each image in Figs. 4(b)–4(h) and 5(b)–5(h), the sample values in $[\mathrm{Min}, \mathrm{Max}]$ on $\mathcal{L}$ are rescaled into $[0 \text{ (black)}, 255 \text{ (white)}]$.

5 Conclusion

In this paper, for sign ambiguity resolution in (4), first we have formulated a minimization problem for a certain energy of local change of the unwrapped phase (Problem 1). Second we reformulated this combinatorial optimization problem on signs into an equivalent constrained binary optimization problem on sign changes (Problem 2). Third, inspired by Goldstein's combinatorial approach to 2D phase unwrapping, we proposed a branch cut type algorithm for the constrained binary optimization problem. The proposed method can efficiently construct an approximate solution of the original combinatorial optimization problem. Numerical experiments demonstrate that the proposed method provides a remarkable improvement over a state-of-the-art method especially around the edges of objects.

Acknowledgment

This work was supported in part by JSPS Grants-in-Aid Grant Numbers 26-920 and B-15H02752.

References

[1] D. Malacara, *Optical Shop Testing*, 3rd ed. New York, NY: Wiley, 2007.

[2] S. S. Gorthi and P. Rastogi, "Fringe projection techniques: Whither we are?," *Optics and Lasers in Engineering*, vol. 48, no. 2, pp. 133–140, Feb. 2010.

[3] S. Zhang, "Recent progresses on real-time 3D shape measurement using digital fringe projection techniques," *Optics and Lasers in Engineering*, vol. 48, no. 2, pp. 149–158, Feb. 2010.

[4] F. Lilley, M. J. Lalor, and D. R. Burton, "Robust fringe analysis system for human body shape measurement," *Optical Engineering*, vol. 39, no. 1, pp. 187–195, Jan. 2000.

[5] L. C. Chen and C. C. Huang, "Miniaturized 3D surface profilometer using digital fringe projection," *Measurement Science and Technology*, vol. 16, no. 5, pp. 1061–1068, Mar. 2005.

[6] K. Genovese and C. Pappalettere, "Whole 3D shape reconstruction of vascular segments under pressure via fringe projection techniques," *Optics and Lasers in Engineering*, vol. 44, no. 12, pp. 1311–1323, Dec. 2006.

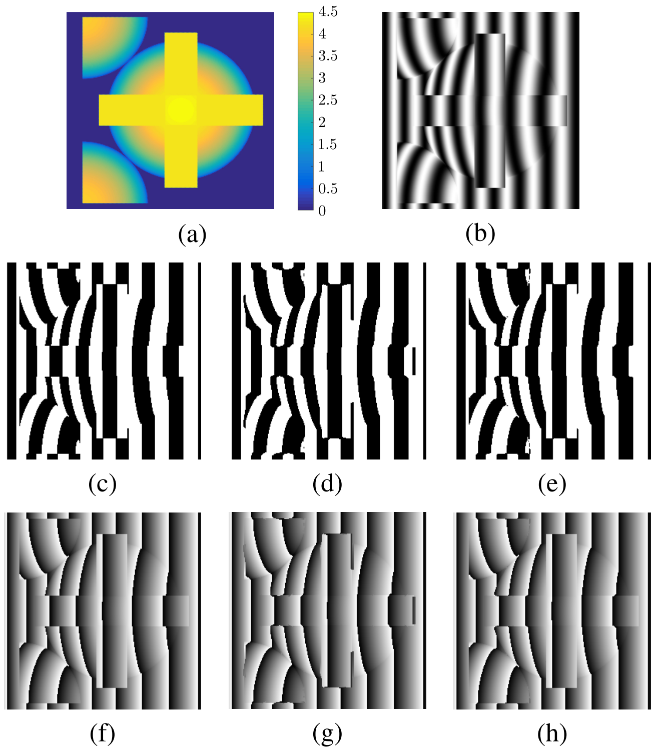

Figure 4: Experimental results (I): (a) object, (b) $I(x,y)$, (c) $s(x,y) = \mathrm{sgn}(W(\phi(x,y)))$ (to be estimated), (d) signs estimated by [23], (e) signs estimated by the proposed sign estimator, (f) $W(\phi(x,y))$, (g) $\phi^W(x,y)$ based on (d), and (h) $\phi^W(x,y)$ based on (e).

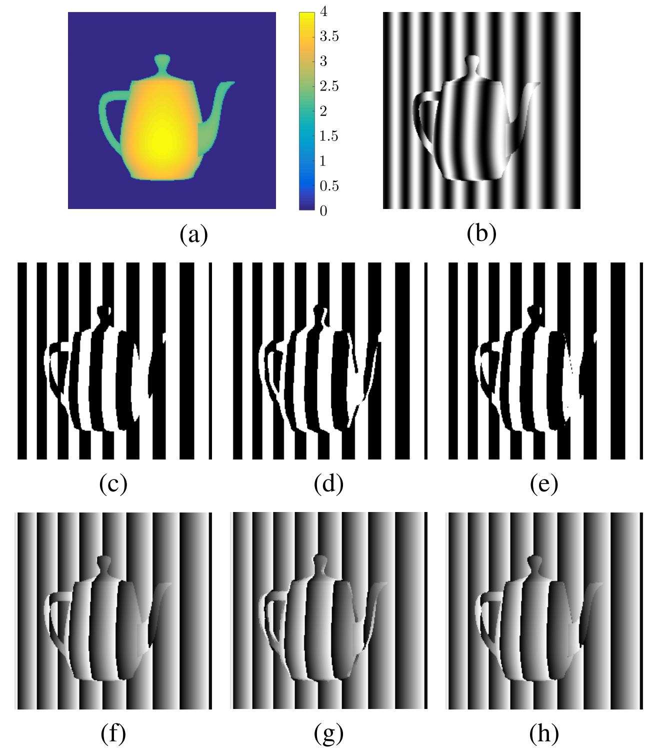

Figure 5: Experimental results (II): (a) object, (b) $I(x,y)$, (c) $s(x,y) = \mathrm{sgn}(W(\phi(x,y)))$ (to be estimated), (d) signs estimated by [23], (e) signs estimated by the proposed sign estimator, (f) $W(\phi(x,y))$, (g) $\phi^W(x,y)$ based on (d), and (h) $\phi^W(x,y)$ based on (e).

[7] M. de Angelis, D. de Nicola, P. Ferraro, A. Finizio, and G. Pierattini, "Liquid refractometer based on interferometric fringe projection," *Optics Communications*, vol. 175, no. 4–6, pp. 315–321, Mar. 2000.

[8] C. Quan, C. J.Tay, X. Y. He, X. Kang, and H. M. Shang, "Microscopic surface contouring by fringe projection method," *Optics and Lasers in Engineering*, vol. 34, no. 7, pp. 547–552, Oct. 2002.

[9] J. Burke, T. Bothe, W. Osten, and C. F. Hess, "Reverse engineering by fringe projection," in *Proceedings of SPIE, Interferometry XI: Applications*, 2002, pp. 312–324.

[10] S. Tan, D. Song, and L. Zeng, "A tracking fringe method for measuring the shape and position of a swimming fish," *Optics Communications*, vol. 173, no. 1–6, pp. 123–128, Jan. 2000.

[11] F. Yuan, D. Song, L. Zeng, "Measuring 3D profile and position of a moving object in large measurement range by using tracking fringe pattern," *Optics Communications*, vol. 196, no. 1–6, pp. 85–91, Sep. 2001.

[12] J. Yagnik, G. S. Siva, K. R. Ramakrishnan, and L. K. Rao, "3D shape extraction of human face in presence of facial hair: A profilometric approach," in *Proceedings of IEEE Region 10 International Conference (TENCON)*, 2005, pp. 1–5.

[13] S. Huang, Z. Zhang, Y. Zhao, J. Dai, C. Chen, Y. Xu, E. Zhang, L. Xie, "3D fingerprint imaging system based on full-field fringe projection profilometry," *Optics and Lasers in Engineering*, vol. 52, pp. 123–130, Jan. 2014.

[14] K. Creath, "Phase-measurement interferometry techniques," *Progress in Optics*, vol. 26, pp. 349–393, 1988.

[15] D. C. Ghiglia and M. D. Pritt, *Two-Dimensional Phase Unwrapping: Theory, Algorithms, and Software*. New York, NY: Wiley, 1998.

[16] L. Ying, "Phase unwrapping," in *Wiley Encyclopedia of Biomedical Engineering, 6-Volume Set*, M. Akay, Ed. New York, NY: Wiley, 2006.

[17] R. M. Goldstein, H. A. Zebker, and C. L. Werner, "Satellite radar interferometry: Two-dimensional phase unwrapping," *Radio Science*, vol. 23, no. 4, pp. 713–720, Jul./Aug. 1988.

[18] D. Kitahara and I. Yamada, "Algebraic phase unwrapping based on two-dimensional spline smoothing over triangles," *IEEE Transactions on Signal Processing*, vol. 64, no. 8, pp. 2103–2118, Apr. 2016.

[19] D. Wu and K. L. Boyer, "Sign ambiguity resolution for phase demodulation in interferometry with application to prelens tear film analysis," in *Proceedings of IEEE Conference on Computer Vision and Pattern Recognition (CVPR)*, 2010, pp. 2807–2814.

[20] M. Servin, J. L. Marroquin, and F. J. Cuevas, "Demodulation of a single interferogram by use of a two-dimensional regularized phase-tracking technique," *Applied Optics*, vol. 36, no. 19, pp. 4540–4548, Jul. 1997.

[21] J. A. Quiroga, M. Servin, and F. J. Cuevas, "Modulo 2π fringe orientation angle estimation by phase unwrapping with a regularized phase tracking algorithm," *Journal of the Optical Society of America A: Optics, Image Science, and Vision*, vol. 19, no. 8, pp. 1524–1531, Aug. 2002.

[22] C. J. Tay, C. Quan, F. J. Yang, and X. Y. He, "A new method for phase extraction from a single fringe pattern," *Optics Communications*, vol. 239, no. 4–6, pp. 251–258, Sep. 2004.

[23] J. Villa, I. De la Rosa, G. Miramontes, and J. A. Quiroga, "Phase recovery from a single fringe pattern using an orientational vector-field-regularized estimator," *Journal of the Optical Society of America A: Optics, Image Science, and Vision*, vol. 22, no. 12, pp. 2766–2773, Dec. 2005.

[24] H. Wang and Q. Kemao, "Frequency guided methods for demodulation of a single fringe pattern," *Optics Express*, vol. 17, no. 17, pp. 15118–15127, Aug. 2009.

[25] C. Tian, Y. Yang, D. Liu, Y. Luo, and Y. Zhuo, "Demodulation of a single complex fringe interferogram with a path-independent regularized phase-tracking technique," *Applied Optics*, vol. 49, no. 2, pp. 170–179, Jan. 2010.

[26] J. A. Quiroga, J. A. Gómez-Pedrero, and Á. García-Botella, "Algorithm for fringe pattern normalization," *Optics Communications*, vol. 197, no. 1–3, pp. 43–51, Sep. 2001.

[27] J. O. Ramsay and B. W. Silverman, *Functional Data Analysis*, 2nd ed. New York, NY: Springer, 2005.